Earth and Planetary Science Letters 289 (2010) 11–21

Contents lists available at ScienceDirect

Earth and Planetary Science Letters

journal homepage: www.elsevier.com/locate/epsl

Integrated climate model-oxygen isotope evidence for a North American monsoon during the Late Cretaceous

Henry C. Fricke [a,*], Brady Z. Foreman [b], Jacob O. Sewall [c]

[a] Colorado College, Department of Geology, Colorado Springs, CO, 80903, USA
[b] University of Wyoming, Department of Geology and Geophysics, Laramie, WY, 82071, USA
[c] Kutztown University of Pennsylvania, Department of Physical Sciences, Kutztown, PA, 19530, USA

ARTICLE INFO

Article history:
Received 26 January 2009
Received in revised form 22 July 2009
Accepted 13 October 2009
Available online 18 November 2009

Editor: P. DeMenocal

Keywords:
oxygen isotopes
monsoon
paleoclimate
Campanian
AGCM

ABSTRACT

During the Late Cretaceous, western North America was characterized by a close geographic association between the Sevier highlands and the Western Interior Seaway. In this paper, an atmospheric general circulation model (AGCM) is used to simulate the impact of this geographic association on surface pressure, wind direction, and precipitation, and it is predicted that seasonal changes in these variables resulted in a strong monsoon along the eastern flank of the Sevier Highlands. Confirmation that these model simulations are accurate is provided by isotopic data from foreland basin sediments. In particular oxygen isotope records from different environments (large rivers, small streams and ponds) and proxies (unionid bivalve shells and paleosol carbonates) indicate that foreland basin streams were recharged by local precipitation with high oxygen isotope ratios while large trunk rivers were recharged by high-elevation precipitation. This hydrologic pattern is observed from Alberta to Utah and is consistent with east to west monsoonal air mass movements and associated seasonal rainfall. Recognition of a highland-driven monsoon has implication in regard to studies of fossil taphonomy, of water vapor transport, and of links between climate and mountain uplift and exhumation in this region.

1. Introduction

Monsoons are characterized by prevailing winds that reverse direction seasonally in response to local pressure changes. Those pressure changes are frequently the result of differential heating and cooling of large, elevated land masses and adjacent oceans. Strong flow towards and up large, elevated land masses often results in vigorous precipitation that can represent a significant percentage of annual rainfall within a region. The Indian monsoon associated with the Tibetan plateau is perhaps the best known, as are the likely influences of that monsoon on a wide variety of long-term geologic processes. For example, intense monsoonal precipitation on the flanks of the Himalayan orogeny has been linked to high rates of chemical weathering and thus drawdown of atmospheric CO_2 and global temperature change (Raymo and Ruddiman, 1992), and to high rates of tectonic exhumation (Willett, 1999; Wobus et al., 2003).

Less intense monsoons also occur in western North America at the present time. In this case, warming of mountains in the Cordillera and Colorado Plateau during summer months produces a ridge of low atmospheric pressure that draws in moisture-laden air in from the Gulf of Mexico. These air masses then interact with those associated with westerly trade winds from the Pacific, and northerly jet streams originating in the Arctic (Bryson and Hare, 1974; Reiter and Tang, 1984).

What is not as well known is the evolution of this North American monsoon over geologic time. The history of Mesozoic and Cenozoic mountain building in western North America is long and complex, however, there were time periods in the past where similar monsoonal patterns likely existed. In particular, inland seaways and/or pronounced embayments in the area that is now the Great Plains immediately to the east of Sevier and Laramide uplifts should have provided ideal conditions for seasonally reversing, zonal movement of air masses, and more importantly water vapor, during these time periods. Indeed east-to-west wind patterns consistent with monsoons have been predicted for the Paleogene and middle Cretaceous in both global and regional climate models (e.g. Poulsen et al., 1999; Kump and Slingerland, 1999; DeConto et al., 1999; Sewall et al., 2000; Sewall and Sloan, 2006; Poulsen et al. 2007). Moreover, large amounts of presumably monsoonal rainfall (~1.5 m) have been inferred for the Front Range of Colorado during the Paleocene based on paleobotanical data (Johnson and Ellis, 2002). In all of these cases, however, direct evidence for monsoonal circulation is lacking.

In this paper, we take an integrated modeling-geochemical approach to studying monsoonal circulation and its influence on foreland basin hydrology during the late Cretaceous of western North America. An atmospheric general circulation model (AGCM)

* Corresponding author. Tel.: +1 719 389 6514; fax: +1 719 389 6910.
E-mail address: hfricke@colorado.edu (H.C. Fricke).

0012-821X/$ – see front matter © 2009 Elsevier B.V. All rights reserved.
doi:10.1016/j.epsl.2009.10.018

simulation for the Campanian epoch suggests that seasonal changes in surface pressure, wind direction, and precipitation consistent with a strong monsoon should have existed along the eastern flank of the Sevier Highlands at this time. Confirmation that these simulations are accurate is provided by oxygen isotope data from foreland basin sediments. Coeval stable isotope records from multiple environments (large rivers, small streams and ponds) and proxies (unionid bivalve shells and paleosol carbonates) are used to create oxygen isotope maps for transects across the Late Cretaceous foreland basin. The observed pattern in oxygen isotope ratios provides empirical evidence that east to west monsoonal air mass movements and associated seasonal rainfall did occur over a large part of western North America at this time.

2. Geologic setting

This study focused on terrestrial sedimentary rocks deposited along the western margin of the Western Interior Seaway (WIS) of North America during the Campanian epoch of the Cretaceous period (83.5 to 70.6 Ma; Gradstein et al., 2004). During this time period, convergent tectonic activity along the Pacific margin of North America resulted in the formation of a north-south trending region of thin-skinned thrust faulting and deformation in what is now the western United States (fold and thrust belt of the Sevier orogeny; DeCelles, 2004; Fig. 1). To the east of this region were foreland basins characterized by alluvial and coastal plain sedimentation, as well as large regions of marine deposition within an epicontinental seaway (Fig. 1). Beginning at ~70 Ma the style of deformation changed, with high-angle reverse faulting and uplift occurring further to the east in a spatially and temporally discontinuous manner (Laramide orogeny; Dickinson et al., 1988; DeCelles, 2004).

2.1. Fossil localities

The unionid bivalves studied here are derived from nonmarine sediments of the Dinosaur Park (DPF), Two Medicine (TMF), Judith River (JRF), Mesa Verde (MVF), and Kaiparowits (KAF) Formations. The sample sites span paleolatitudes 45°N to 57°N, and are located at variable distances from the paleoshoreline of the WIS (Fig. 1). Sample sites from the DPF, JRF, and MVF were likely within a few tens of kilometers from the coastline, whereas TMF and KAF sample sites were likely over 200 km away (Heydenburg, 1966; Hippe et al., 1986; Eberth and Hamblin, 1993; Rogers, 1998; Rogers and Kidwell, 2000; Roberts, 2007; Rogers and Brady, in press). Temporally, the sample sites are tightly constrained. Radiometrically-dated bentonites (^{40}Ar/^{39}Ar of sanidine crystals) in the TMF, JRF, and KAF bracket the ages of the sample sites between 77.5–74.3 Ma, 75.4–74.5 Ma, and 76.1–74.0 Ma, respectively (Rogers et al., 1993; Roberts et al., 2005; Foreman et al., 2008). A combination of mammalian biostratigraphy, paleomagnetic data, and radiometric dates from bentonites in the DPF indicate these sample sites are ~76.5–75 Ma (Dettman and Lohmann, 2000 and references therein). The Wyoming MVF sample site is the least constrained, but was collected in the 'upper sequence' of the Parkman Sandstone member in the MVF of Heydenburg (1966). This member is lithostratigraphically equivalent to the lower JRF (~80–75.4 Ma) (Gill and Cobban, 1973; Rogers et al., 1993; Rogers, 1993). Indeed, the Parkman Member directly interfingers with lower JRF strata in Montana (Gill and Cobban, 1973; Rogers, 1998). Thus all sample sites in this study are 76 ± 2 Ma.

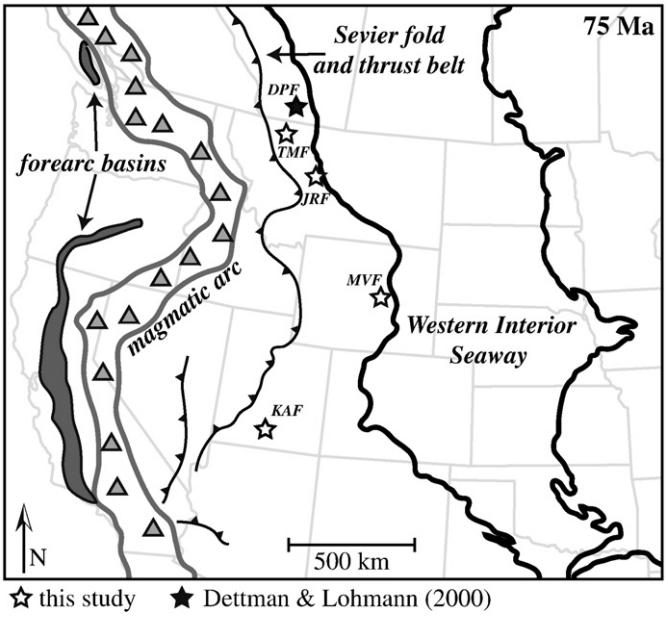

Fig. 1. Campanian paleogeographic map of the Western Interior showing sample sites. Major tectonic features from Dickinson (2004) and approximate location of the seaway from Blakey (2008).

The TMF and KAF represent deposition in an up-dip alluvial plain. The TMF is dominated by fluvial sandstones of braided and meandering origin and various interchannel facies including well-developed, carbonate nodule-bearing, paleosol horizons and rare but widespread lacustrine intervals (Rogers, 1998). In contrast, the KAF is dominated by fluvial sandstone representative of suspended-load channels in meandering river systems as well as overbank deposits composed predominantly of thick pond facies and hydromorphic paleosols (Roberts, 2007). The DPF, JRF, and MVF represent deposition in coastal plain environments and are composed of tidally influenced fluvial sandstones, carbonaceous pond and backwater facies, paleosols displaying hydromorphic features, and shoreface sandstones, which in some cases directly interfinger with nearshore marine strata of the WIS (Heydenburg, 1966; Hippe et al., 1986; Eberth and Hamblin, 1993; Rogers, 1998; Rogers and Kidwell, 2000; Roberts, 2007). Unionid bivalves from the formations were recovered from distinct facies associations, which can be divided into three basic depositional environments, 1) large or 'trunk' rivers, 2) streams, and 3) ponds.

Large river facies are laterally extensive (many tens to hundreds of meters), sheet-like fluvial sandstones. They are characteristically thick (2.5 to 10+ meters thick) and composed of various scales of cross-bedding (Heydenburg, 1966; Rogers, 1998; Rogers and Kidwell, 2000; Roberts, 2007; Rogers and Brady, in press). In addition, these fluvial sandstones are multi-storied, indicating multiple reoccupation events by the active channel to the area. Thus these deposits represent major thoroughfares for water and sediment in the basin system. In contrast, stream facies are single-storied, lenticular in geometry, display small-scale cross-bedding, limited to a few meters in thickness, and laterally extend only tens of meters. They are commonly associated with siltstone lenses and tabular silty mudstones containing carbonized plant material, root traces, burrows, and vertebrate/invertebrate remains (Rogers, 1990). These facies represent various channel abandonment (e.g. oxbow lake) and interchannel environments (Rogers, 1990). Their single-storied nature, smaller overall geometries, and abundant evidence for abandonment events suggest these streams were smaller, more transitory features, and relatively minor pathways for water and sediment within the basin system as compared to large rivers. Pond facies are composed of tabular silty claystones and clay-rich siltstones (Rogers and Kidwell, 2000; Roberts, 2007; Rogers and Brady, in press). Pond deposits are typically around one meter in thickness and can extend laterally for up to 100 m or more before becoming obscured by vegetation. The deposits are light brownish-grey to olive grey in color and massive to weakly laminated in structure. The deposits are commonly carbonaceous, with carbon occurring mostly as horizontal laminations, but also as scattered accumulations and as fossil wood. Oxidized root traces,

amber blebs, carbonized seeds, and scattered green claystones are also present in some deposits, as are vertebrate and invertebrate remains (Rogers and Kidwell, 2000; Roberts, 2007; Rogers and Brady, in press).

3. Methods and results

3.1. Global climate modeling

We used the National Center for Atmospheric Research (NCAR) Community Atmosphere Model (CAM; Collins et al., 2006) to conduct a fixed lower boundary condition, atmosphere only simulation of the Campanian. CAM contains 26 vertical levels and our simulations were conducted at a horizontal resolution of spectral T42 (~2.8° latitude × 2.8° longitude). Campanian geography, topography, and vegetation were modified from previously published Cretaceous boundary conditions (Otto-Bliesner et al., 2002; Sewall et al., 2007) and are presented in Fig. 2, and a monthly varying seasonal cycle of sea surface temperatures (SST) was developed from an equilibrated, fully coupled Campanian simulation of the NCAR Climate System Model (CSM v. 1.4) (Otto-Bliesner et al., 2002). Atmospheric pCO_2 was specified at 1680 ppm, pCH_4 at 700 ppb, and pN_2O at 275 ppb similar to the driving conditions associated with our SST distribution (Otto-Bliesner et al., 2002). Orbital parameters were specified at modern values and the solar constant was reduced to 1355 W/m^2. Our simulation was integrated for 30 model years and the final 10 years of the equilibrated simulation (global average surface temperature trends for the last decade were −0.0091 °C) were averaged for analyses.

Our simulated Campanian climate indicates a strong annual cycle in both surface temperatures and pressures over the Sevier Highlands (not shown). Temperatures over the highlands begin warming from winter lows (~3 °C over the highest peaks in December and January) in April and peak in July and August (~23 °C over the highest peaks). Local sea level pressure declines with increasing temperature and a minimum of 1002 mb over the highest peaks and 990 mb over the foreland is reached in July, down from a January high of 1022 mb over the highest peaks and 1015 mb in the foreland. This strong seasonality of surface temperatures and pressures supports a robust, local

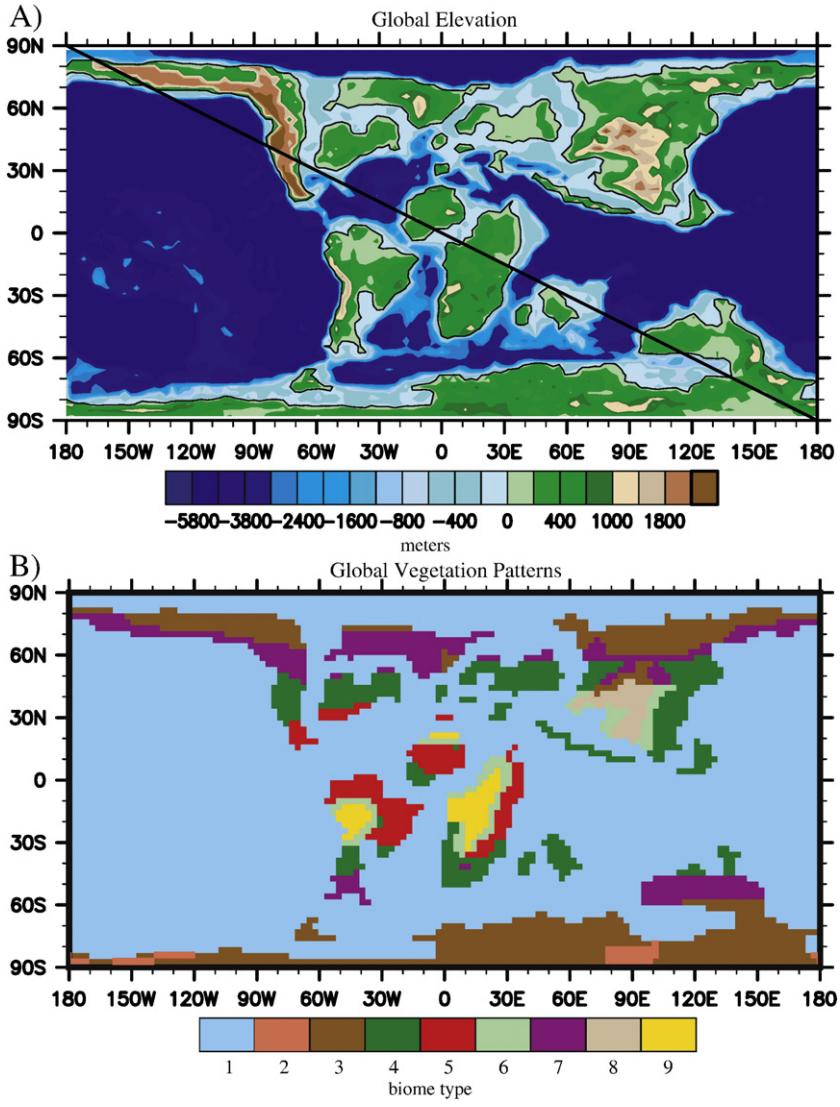

Fig. 2. Surface boundary conditions for the Campanian (~80 Ma) AGCM simulation. A) Geography, topography, and bathymetry. Elevations in meters above (greens and browns) and below (blues) sea level. Darker blues are deep water, lighter blues are shallow. Lower elevation land is green, higher elevations are brown. The contour interval is greatest at the color bar extremes and smaller near the land/sea boundary. B) Global vegetation distribution represented as generalized biomes. 1 = ocean, 2 = Closed canopy, deciduous, needle leaved forest, 3 = Closed canopy, evergreen, needle leaved forest, 4 = Closed canopy, deciduous, broad leaved forest, 5 = Moist savanna: low, dense understory with limited, deciduous overstory, 6 = Dry savanna: low, sparse understory with limited, evergreen overstory, 7 = Open canopy mixed forest with shrub understory, 8 = Scrub forest: dense, deciduous shrublands, 9 = Semi desert: sparse, deciduous shrublands.

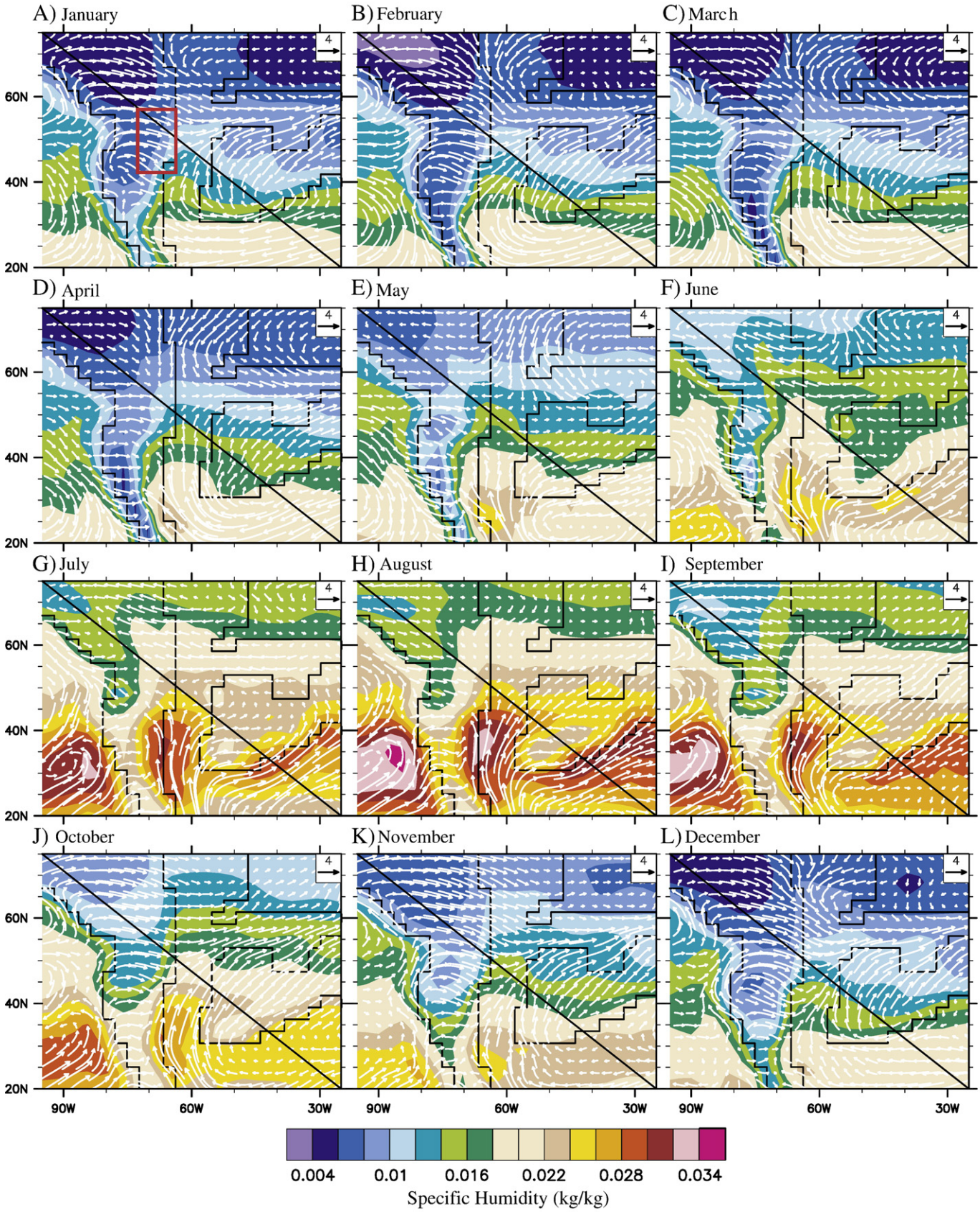

Fig. 3. Simulated Campanian surface winds (white vectors; m/s) and specific humidity (colored contours; kg/kg) over North America (continental outlines in solid black) for A) January, B) February, C) March, D) April, E) May, F) June, G) July, H) August, I) September, J) October, K) November, and l) December. In spring, summer, and early fall, south, southeasterly winds bring abundant moisture into the Sevier highlands and foreland. Winter and early spring are characterized by westerly flow and drier conditions in the Sevier highlands and foreland. The red box in A) represents the sampling area and the area for which precipitation results are presented (Fig. 4).

monsoon with generally westerly winds in the colder months being replaced by south, southeasterly flow in the spring, summer, and early fall (Fig. 3). The south southeasterly warm season phase of this monsoon transports abundant moisture off of the WIS and into the Sevier foreland and highlands (Fig. 3). Orographic lifting of these moist air masses results in abundant, convective precipitation with the Campanian sampling localities (see Fig. 1 and box in Fig. 3A) receiving 77% of their total annual precipitation in the form of convective precipitation with 77% of that convective precipitation (59% of the annual total) arriving between the months of April and August. Complete precipitation results for the region bounded by the box in Fig. 3A are presented in Fig. 4.

3.2. Oxygen isotope analysis

Isotopic data from unionid bivalves represents a mix of new results and a compilation of data from previous studies. A portion of the bivalve and all the paleosol carbonate data presented here from the TMF and JRF were first published in Fricke et al. (2008), while bivalve data from the DPF is derived from Dettman and Lohmann (2000). New isotopic data from JRF and TMF invertebrates were obtained using an automated carbonate preparation device (KIEL-III) coupled to a Finnigan MAT 252 isotope ratio mass spectrometer at the University of Arizona and using a Finnigan MAT 253 isotope ratio mass spectrometer housed in the Department of Geological Sciences at the University of Michigan. Isotope data from the MVF and KAF was obtained using a Thermo Finnigan Delta^{PLUS} XP Continuous Flow isotope ratio mass spectrometer housed at the University of Wyoming Stable Isotope Facility. Bivalves were rinsed multiple times with distilled water, drilled near the umbo, and roasted at 200 °C prior to reaction at ~77 °C with anhydrous phosphoric acid and introduction to the mass spectrometer. Mineralogical analysis of invertebrate shell material was conducted using a Phillips 1710 X-ray diffractometer at Colorado College and a PANalytical X'Pert PRO PW3040 X-ray diffractometer at Macalester College. Stable isotope ratios are reported as $\delta^{18}O$ and $\delta^{13}C$ values, where $\delta = (R_{sample}/R_{standard} - 1) * 1000‰$, and the standard is VPDB. These isotope ratio measurements are normalized based on repeated measurements of NBS-19, NBS-18 and in-house powdered carbonate standards. Analytical precision is $\pm 0.1‰$ for both $\delta^{18}O$ and $\delta^{13}C$ (1σ). All data are available in the online Supplementary material.

Before discussing patterns of isotopic data (below) it is necessary to address the question of diagenesis. Fricke et al. (2008, 2009) provide a detailed diagenetic evaluation of fossil material from the TMF, JRF, DPF, and KAF sample sites using isotopic and mineralogic data from a number of different taxa. In particular, carbon and oxygen isotope offsets among bivalves, paleosol carbonates and other associated vertebrate taxa (freshwater fish and dinosaurs) indicate that primary paleoecological information is preserved in bivalve and other fossil material (Fricke et al., 2008, 2009). Our mineralogical analysis of a subsample of unionid bivalve shells from each formation is consistent with this result, as X-ray diffraction indicates they are composed of aragonite (>99%). Moreover, shells display a mother-of-pearl luster and well-preserved growth laminae under light microscope. Because aragonite easily alters to calcite during minimal diagenesis, and these samples maintain an aragonite mineralogy, substantial isotopic alteration is not likely.

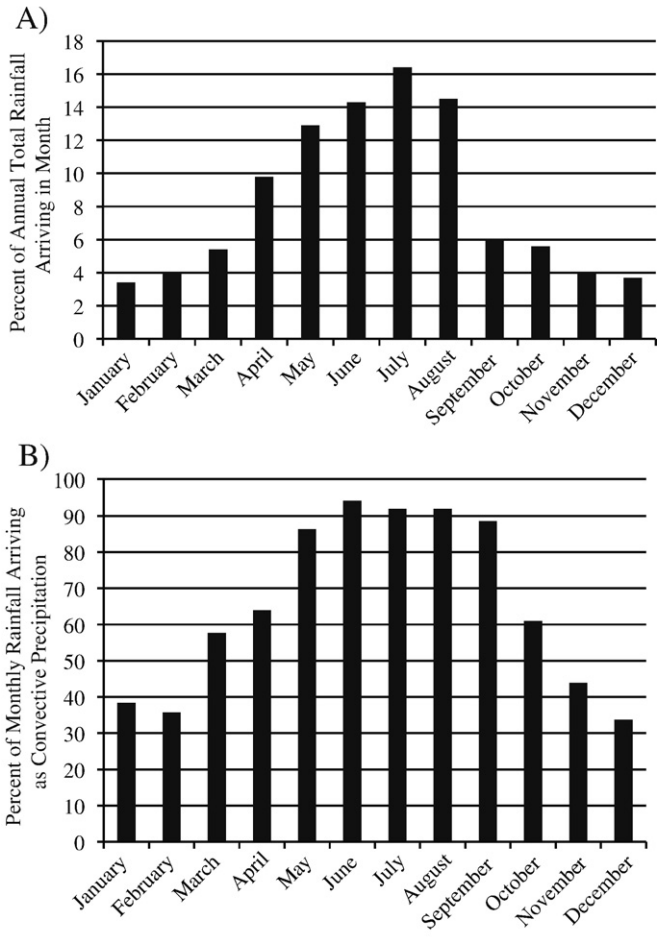

Fig. 4. Simulated Campanian precipitation totals over the bounding box shown in Fig. 3A. The south, southeasterly flow of the summer monsoon (Fig. 3) exerts substantial control on annual precipitation patterns in this region. The proportion of annual rainfall arriving in a given month (A) rises through the spring and into the summer, peaking in July. In these months, south, southeasterly winds off the WIS force moist air up the front of the Sevier highlands and promote vigorous convective precipitation; as the proportion of annual rainfall arriving in a given month rises, so does the proportion of that rainfall that arrives as convective precipitation (B).

4. Discussion

Wind and precipitation patterns inferred from the AGCM simulations are indicative of a strong Campanian monsoon. A bimodal distribution of oxygen isotope data from foreland basin samples provides evidence for high-elevation river recharge to the west and low-elevation river recharge to the east that supports this interpretation, as do other geologic observations of foreland basin rocks.

4.1. Model characterization of the Campanian monsoon

Strong monsoons and associated seasonal precipitation signatures have been produced in previous simulations of relatively young orogenies and proximal ocean bodies (e.g. Ruddiman and Kutzbach, 1989; Kutzbach et al., 1989; Sewall et al., 2000; Zhisheng et al., 2001; Sewall and Sloan, 2006; Poulsen et al., 2007). Although the growth and evolution of the Asian monsoon in conjunction with late Cenozoic uplift of the Tibetan plateau (e.g. Zhisheng et al., 2001) is likely the best know tectonically driven monsoon, middle Cretaceous simulations of Poulsen et al. (2007) and early Paleogene simulations of Sewall et al. (2000) and Sewall and Sloan (2006) are most comparable to our Campanian simulation. Poulsen et al. (2007) found that increasing elevation of the ancestral Rocky Mountains in western North America greatly enhances precipitation totals on the windward/eastward side of the mountains. Sewall et al. (2000) and Sewall and Sloan (2006) found that high elevations of the Laramide orogeny drove vigorous south, southeasterly summer flow off of the Mississippi Embayment that transported abundant moisture to the Laramide front where orographic lifting drove deposition of that moisture as convective precipitation. Similarly, in our Campanian simulation, high elevations (average elevations of the core highlands

are ~2000 m; Fig. 2) of the Sevier orogeny warm rapidly in the spring and summer, promoting local reductions in pressure (not shown) and supporting south, southeasterly flow off of the WIS (Fig. 3). Onshore/westward flow is a persistent feature south of ~30° N latitude (Fig. 3) but begins to spread northwards in the spring, reaching 40° N latitude in April (Fig. 3D) and onshore flow is persistent as far as 75° N latitude in June and July (Fig. 3F and G) before weakening in August and returning to generally offshore flow north of ~35° N latitude in September (Fig. 3H and I).

The proximity of the Sevier highlands to the WIS gives the Sevier front monsoon a robust precipitation signature as well. In contrast to cool season westerly winds that deposit much of their moisture on the western flank of the uplift leaving the Sevier front and foreland in a rain shadow (not shown), warm season southeasterly winds off the WIS deliver moisture directly from the seaway to the Sevier foreland and front. This direct moisture delivery accounts for 77% of the annual rainfall in the sampling region (see box in Fig. 3A) with most of the late spring and summer rainfall arriving as convective precipitation (Fig. 4). In addition to the seasonally reversing circulation, this strong seasonality of precipitation source, amount, and type is one of the most prominent climatological features of the sampled stretch of the Sevier front.

4.2. $\delta^{18}O$ characterization of the Campanian monsoon

4.2.1. $\delta^{18}O$ of river waters and regional hydrology

Oxygen isotope ratios of rivers (and streams and ponds) can be used to infer seasonal east to west air mass movement and the monsoonal precipitation patterns described above because they provide information on the source of river recharge and on the rainout history of air masses that are the source of this recharge. In general, $\delta^{18}O$ of rivers represents a temporally- and spatially-averaged sample of catchment-wide meteoric precipitation. The degree of $\delta^{18}O$ spatial-averaging depends on the 'drainage order' of the stream from which ancient samples are derived (i.e. catchment size, mean elevation and topography of the watershed, and the elevation-dependent changes in amount of precipitation) (Rowley, 2007). Smaller rivers and streams are recharged primarily by local precipitation and, thus, have $\delta^{18}O$ more similar to local precipitation, while larger rivers are recharged by a combination of local precipitation and distal/upland precipitation and $\delta^{18}O$ values are representative of both sources.

To investigate sources of river recharge and patterns of air mass movement, it is necessary to compare $\delta^{18}O$ of river water between small and large rivers in the same area, or between similar sized rivers in different areas. Such a comparison can be fruitful because $\delta^{18}O$ of the precipitation that recharges these river systems can vary significantly in response to the hydrological/rainout 'history' of air masses that are supplying precipitation to these surface water reservoirs. The primary cause of isotopic variability in precipitation is the temperature-controlled fractionation of ^{18}O into condensate as water is precipitated and removal of this water from cooling air masses (Dansgaard, 1964; Rozanski et al., 1993). The resulting patterns in oxygen isotope ratios of precipitation include a regular decrease as air masses cool while rising over mountains, moving away from coastal areas, and moving from warmer, lower latitude source areas to cooler, polar sinks (Dansgaard, 1964; Rozanski et al., 1993; Gat, 1996).

One pertinent example of these isotope-hydrology relations comes from large rivers draining the North American Cordillera and Himalayan mountains that have $\delta^{18}O$ much lower than local precipitation in their lower elevation reaches due to contribution of drainage from high elevation areas (Dutton et al., 2005; Rowley, 2007; Kohn and Dettman, 2007). A second example is the pattern in $\delta^{18}O$ of precipitation associated with monsoonal systems in southeast Asia (Araguas-Araguas et al., 1998) where eastward-moving air masses having invariant mean annual $\delta^{18}O$ from the coast (e.g. Hong Kong, 65 m, $\delta^{18}O = -6.5$ ‰) to low-elevation sites several hundred kilometers inland (e.g. Guilin; 170 m, $\delta^{18}O = -6.1$‰) before decreasing rapidly as elevation begins to increase (e.g. Guiyang; 1071 m, $\delta^{18}O = -8.3$‰; Kunming, 1841 m, $\delta^{18}O = -10.4$‰; Lhasa, 3949 m, $\delta^{18}O = -15.3$‰).

4.2.2. Estimating $\delta^{18}O$ of foreland basin surface waters

In order to study the hydrology of the Cretaceous foreland basin using similar kinds of oxygen isotope comparisons, material was sampled from several kinds of depositional environments (rivers, streams, ponds and floodplains) and from multiple locations that span an ~250 km east-west transect and ~15° of latitude (Fig. 1). $\delta^{18}O$ of surface water ($\delta^{18}O_w$) was estimated using $\delta^{18}O$ of bivalve shell aragonite and nodular calcite. Different approaches to doing this for bivalves were reviewed by Kohn and Dettman (2007). They note that growth of shell material occurs primarily between water temperatures of 12 °C and 30 °C, with optimum growth occurring between 20 and 25 °C regardless of how environmental temperatures vary seasonally. The result is a linear relationship between the mean $\delta^{18}O$ of fluvial waters and bulk-sampled $\delta^{18}O$ from unionid shells that has a slope of 0.89 despite a range in mean annual surface temperatures from 3 to 23 °C (Kohn and Dettman, 2007). Because our bulk sampling method incorporates shell material from multiple growth laminae, providing a multi-year average, we have chosen to use this empirical relation of Kohn and Dettman (2007) to estimate $\delta^{18}O$ of Late Cretaceous surface waters (Table 1; Supplementary data). In any case, estimates of $\delta^{18}O$ surface water are relatively insensitive to differences in temperature of aragonite formation, (±4.5 °C corresponds to ±1‰ of aragonite), and thus differences in temperature of aragonite formation alone cannot account for the large range in $\delta^{18}O_w$ inferred from our dataset (see below).

To estimate $\delta^{18}O_w$ using isotopic data from paleosol carbonate nodules of the TMF, temperature estimates made using paleobotanical data are used along with the inorganic calcite fractionation equation of Friedman and O'Neil (1977). In particular it is assumed that nodules formed at either the estimated mean annual temperature of 16 °C (Wolfe and Upchurch, 1987) or the estimated warm month mean temperature of 24 °C (Wolfe and Upchurch, 1987). Because nodules form over many years, these estimates also represent a multi-year average.

After applying these approaches to samples from the DPF, TM, JRF, MVF and KAF, two populations of bivalves are observed that have distinct $\delta^{18}O_w$ values (Fig. 5A). Of these, one group is found exclusively in thick channel sands associated with large rivers and is characterized by very low $\delta^{18}O_w$. In contrast, soil, stream, and most pond estimates of $\delta^{18}O_w$ inferred from paloesol and bivalve carbonates are significantly higher (Fig. 5A). The means of these two groupings do not overlap within two standard deviations, yet within the groupings they do overlap regardless of their geologic formation of origin (Table 1, Fig. 5A, see the Supplementary materials for additional details regarding statistical analysis). Based on the

Table 1
Summary statistics for surface water oxygen isotope compositions (VSMOW scale).

Formation	Depositional environment	Sample size	Mean ± 2?	Median	Range (max/min)
DPF	Large river	128	−17.2 ± 2.8‰	−17.0‰	−14.8‰/−21.3‰
TMF	Stream	7	−8.6 ± 1.5‰	−8.8‰	−7.6‰/−9.7‰
TMF	Soil (at 16 °C)	13	−9.5 ± 1.1‰	−9.4‰	−8.4‰/−10.5‰
TMF	Soil (at 24 °C)	13	−8.2 ± 1.1‰	−8.1‰	−7.0‰/−9.1‰
JRF	Pond (*a*)	6	−7.6 ± 1.0‰	−7.4‰	−7.2‰/−8.3‰
JRF	Pond (*b*)	5	−16.8 ± 0.6‰	−17.0‰	−16.3‰ /−17.0‰
JRF	Large river	19	−16.6 ± 2.8‰	−16.2‰	−13.5‰/−18.7‰
MVF	Stream	3	−14.7 ± 1.5‰	−14.7‰	−14.0‰/−15.5‰
KAF	Pond	6	−8.2 ± 0.9‰	−8.0‰	−7.8‰/−8.9‰
KAF	Large river	8	−16.2 ± 0.5‰	−16.2‰	−16.0‰/−16.7‰

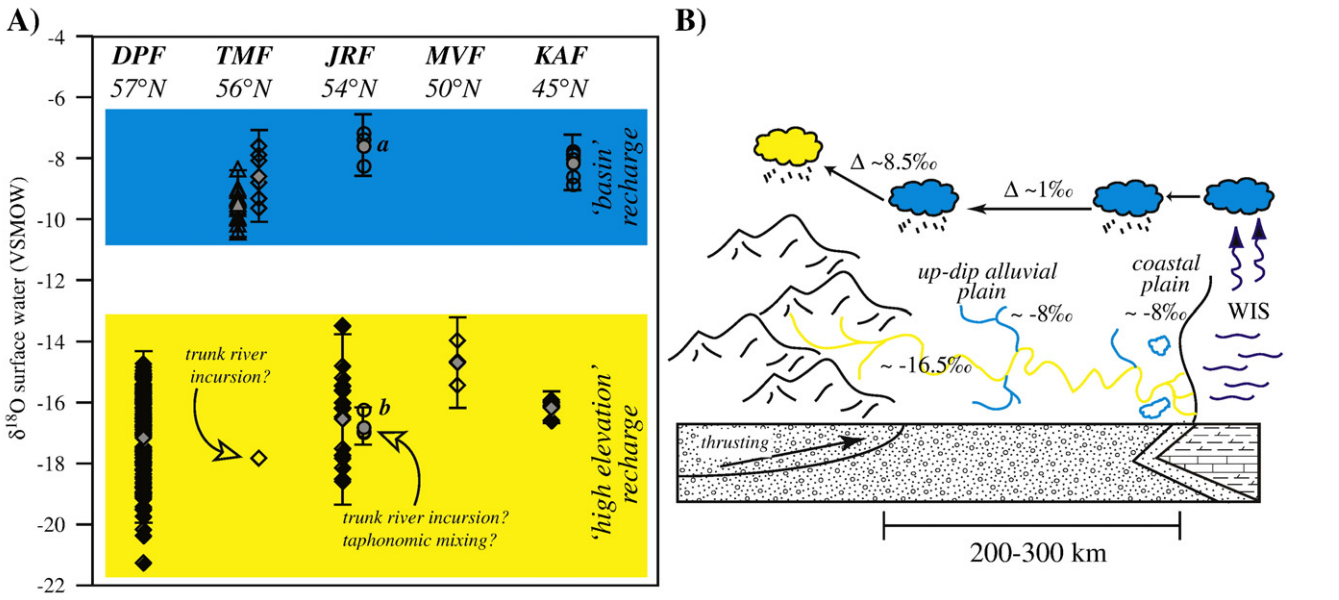

Fig. 5. A. Surface water 3δ^{18}O estimates for each formation and depositional environment (filled diamonds = large 'trunk' rivers; open diamonds = stream facies; open circles = pond facies; open triangles = soil carbonates). Mean values are represented by grey symbols and brackets indicate two standard deviations from the mean. Approximate paleolatitudes for the sample sites are given below the formation abbreviation. '*a*' and '*b*' correspond to JRF pond bivalve data groups in Table 1. Soil carbonates are plotted assuming a temperature of formation of 16 °C. B. Schematic diagram illustrating gross hydrology of the foreland system. Moisture derived from the Western Interior Seaway was transported west across the low-relief basin during the summer months. Rainout was characterized by largely uniform δ^{18}O values, which recharged basin ponds, lakes, small streams, and soil waters. Rainout associated with highlands of the Sevier fold and thrust belt was significantly lower, and recharged large 'trunk' river systems.

sessile behavior of unionid bivalves and the taphonomic evidence suggesting little post-mortem transport (i.e. some sites contain unionids with closed valves and are preserved in life position), these values are thought to largely reflect the δ^{18}O of waters associated with the depositional environment from which the unionids were recovered (Rogers and Kidwell, 2000; Roberts, 2007; Rogers and Brady, in press). However, there are two notable departures from this trend. One bivalve specimen from TMF stream facies had an estimated $\delta^{18}O_w$ of −17.9‰ (not included in group summary statistics). This may be due to a temporary incursion of a large river into stream facies, such as a temporary stream capture, failed avulsion of the trunk river, or related hydrologic event. However, a collection error is also possible. TMF unionids were surface collected and not recovered *in situ*. Unionid shells are exceedingly rare in the multi-storied, large river facies, yet down-slope transport via surface erosion into our 'stream facies' sample site is feasible.

The second departure from the dominant large river vs. pond/stream/soil trend is represented by bimodal estimates of $\delta^{18}O_w$ from JRF ponds. Collection error and down-slope transport is not a factor here as unionids were collected *in situ*. The bimodality of their δ^{18}O values represents either 1) temporary incursion from nearby large trunk rivers into pond waters or 2) post-mortem transport of a subset of the bivalves from fluvial systems into ponds. Both scenarios are feasible given sedimentologic and taphonomic evidence. Pond deposits are laterally extensive and are in many places subjacent to and scoured by thick fluvial sandstones providing definitive evidence for interaction between the two environments (Rogers and Brady, in press). Although not directly observed in the field, it is also feasible that rivers occasionally fed into or spilled-over their banks into low-lying ponds. In this scenario, none of the pond unionids have been transported and the bimodal oxygen isotope values record alternating periods of fluvial vs. pond water dominance. Unionids from the ponds are all shell hash, both disarticulated and fragmentary. This first scenario requires *in situ* destruction of these unionids within the pond environment. Yet, delicate, thin-shelled, high-spired gastropods are unbroken and found within centimeters of unionid material, suggesting that unionid destruction occurred perhaps during transport rather than within the ponds. However, this is difficult to rectify with the fact that all unionid material exists as shell hash in the ponds, not just the shells exhibiting extremely negative δ^{18}O. Regardless of the actual mechanism, both scenarios require interaction between fluvial and pond systems and do not fundamentally change the isotopic interpretations.

4.2.3. δ^{18}O evidence for Campanian monsoon

The bimodal distribution of estimated $\delta^{18}O_w$ and the inferred hydrologic environment associated with different bivalves and paleosol nodules provides support for AGCM simulations that predict a strong east–west monsoon during the Campanian. All bivalves and nodules from soil, stream, and most pond settings have $\delta^{18}O_w$ of ~ −8‰ and these reflect small catchments and groundwaters that were recharged by local precipitation in the JRF, TMF and KAP areas. In the absence of evidence for intense evaporation, δ^{18}O of these streams, ponds and groundwaters is assumed to be similar to that of local precipitation. The implication of these data is that precipitation over both coastal wetlands and alluvial floodplains, ~250 km inland, varied little over the entire low-elevation part of the foreland basin landscape, and that this pattern extended from at least 45 to 55°N paleolatitude. (Fig. 5B). Much lower estimated $\delta^{18}O_w$ values indicate that the hydrology of larger, higher order river systems was different from that of smaller streams, ponds and floodplains, and suggest that they drained larger and higher elevation catchments of the nearby Sevier highlands (Fig. 5B). The fact that river waters with such low δ^{18}O were still present in the JRF, DPF, MVF and KAF formations, several hundred kilometers downstream from their presumed source, indicates that recharge from these high-elevation catchments dominated river recharge.

These isotopic patterns (Fig. 5) are consistent with seasonal (spring and summer) movement of moisture-laden air masses from the WIS westward towards the Sevier highlands as predicted by the AGCM simulations of a strong monsoon (Fig. 3). Under this scenario, δ^{18}O of precipitation is relatively high and uniform during spring/summer transport over the low topographic landscape of the coastal

and alluvial plain regions of the foreland basin. Once air masses reach the Sevier highlands, they rise and cool resulting in enhanced precipitation and significant lowering of precipitation $\delta^{18}O$. This high-elevation precipitation, in turn, recharged the large rivers that flowed to the east over the foreland basin.

4.3. Implications of a Late Cretaceous monsoon in western North America

Global climate model simulations from other time periods and using other models support the hypothesis presented here that having highlands immediately to the west of the Western Interior Seaway during Cretaceous and Paleogene time would have allowed for strong, seasonal winds from the east (Poulsen et al., 1999; Kump and Slingerland, 1999; DeConto et al., 1999; Sewall and Sloan, 2006; Poulsen et al., 2007), and, thus, for a strong seasonal precipitation signature. Similarly, sedimentary, taphonomic ,and paleofloristic data from the foreland basin, all indicate that coastal lowlands were humid and the up-dip alluvial plains were seasonally dry (Jerzykiewicz and Sweet, 1987, 1988; Wolfe and Upchurch, 1987; Carpenter, 1987; Rogers, 1990; Falcon-Lang, 2003). In particular the occurrence of paleosol carbonates and redbeds in TMF are consistent with seasonal/monsoonal rainfall, while growth interruptions in conifer remains point to seasonal drying (Falcon-Lang, 2003). Recognition of strongly seasonal precipitation driven by adjacent highlands has important ramifications for the study of fossil remains, water vapor transport, and tectonic uplift and exhumation. Some of these are described below.

4.3.1. Monsoonal precipitation and fossil taphonomy

Recent investigations of vertebrate fossil assemblages in the Dinosaur Park formation have lead to the suggestion that seasonal flooding of the coast of the WIS was a common occurrence (Eberth and Getty, 2005; Eberth et al., in press). According to this hypothesis, large rivers (35 to 200 m bankfull width and 5–25 m depth; Eberth, 2005) of the coastal plain broke their banks and flooded the entire low-relief landscape. As in modern-day Bangladesh, the prolonged occurrence of standing water that resulted was lethal to herds of large vertebrates, thus explaining the occurrence of 'mega-bonebeds' that are made up of 10 s to 100 s of individuals of the same dinosaur species (Eberth and Getty, 2005; Eberth et al., in press). In the case of fossil localities in the inland, up-dip Two Medicine formation, there is also evidence that bonebed formation is related to highly seasonal variations in rainfall. In these cases, however, taphonomic evidence point to seasonal drying and episodic drought as a likely cause of high mortality (Rogers, 1990, 1998).

The existence of a Campanian monsoon and intense seasonal rainfall is consistent with the taphonomic evidence for seasonal flooding of the coasts and seasonal drought of the upland alluvial plains, and thus provides an explanation for the occurrence of bonebeds in both areas. In particular, $\delta^{18}O$ of large rivers from the DPF have the lowest values observed, which indicate that intense rainout of air masses took place as they moved across the foreland and up the adjacent Sevier highlands during the rainy season, and that this seasonal recharge played a significant, if not major, role in the hydrology of coastal plain settings. Although preliminary, recognition of a link between a seasonal monsoon, taphonomy of vertebrate assemblages, and sedimentological features (width and depth of river channels) may aid in the interpretation of fossil assemblages and sedimentological features in other areas and time periods.

4.3.2. Monsoonal precipitation and models of atmospheric vapor transport

Low $\delta^{18}O$ associated with monsoonal precipitation and foreland basin river recharge along the WIS may also affect studies of vapor and latent heat transport. For example, Ludvigson et al. (1998), White et al. (2001) and Ufnar et al. (2002, 2004) estimated $\delta^{18}O_w$ using paleosol siderite from multiple sites along the coast of the WIS during the mid-Cretaceous, and compared these estimates to present-day $\delta^{18}O_w$ values and to $\delta^{18}O_w$ predicted for the warm Cretaceous using modern empirical temperature-$\delta^{18}O_w$ relationships. They concluded that $\delta^{18}O_w$ values inferred from siderite were ~6 to 13‰ lower than expected given the paleolatitude of the sites. Assuming that these low $\delta^{18}O_w$ values represent zonal (i.e. longitudinal) mean values, mass balance models of the global hydrologic cycle were then used to conclude that the mid-Cretaceous was characterized by enhanced atmospheric water vapor and latent heat transport from low to high latitudes (White et al., 2001; Ufnar et al., 2002, 2004).

Although precipitation was no doubt intense along the foreland basin due to the monsoon circulation described above, a potential problem with mass balance models of the global hydrologic cycle outlined above is that low $\delta^{18}O$ values may only be associated with the north-south trending WIS-foreland basin-highland system, and therefore cannot be used to reflect *zonal* averages. If low $\delta^{18}O$ values inferred from siderite are in fact limited in spatial occurrence, and represent a monsoon, then the degree to which the Cretaceous hydrological cycle and vapor transport was enhanced may be overestimated. Using model predictions of $\delta^{18}O$ of precipitation during the middle Cretacous, Poulsen et al. (2007) found that low $\delta^{18}O$ values occurred primarily in association with high elevation areas of the Western Cordillera, and they reached a similar conclusion that such low values represent regional-scale rather than a zonal-scale processes.

4.3.3. Monsoonal precipitation and exhumation of Sevier uplifts

Our AGCM simulation indicates that the Campanian Sevier front may have experienced monsoonal precipitation on the order of 1.25 m/year. This was enough to dominate the $\delta^{18}O$ of large rivers ~250 km downstream from their source, and raises the interesting possibility that feedbacks existed between tectonic uplift and exhumation, sediment deposition, and climate during the Sevier orogeny. In the case of modern mountains, thermochronologic studies of the Cascade range and the Himalayas indicate that in regions where precipitation is focused, rates of erosion and, thus, tectonic exhumation, are higher than compared to other areas (Willett, 1999; Wobus et al., 2003; Reiners et al., 2003). It has also been suggested that Cenozoic uplift and weathering of the Tibetan plateau led to a decrease in the concentration of CO_2 (pCO_2) in the atmosphere and global cooling, and to an increase in the $^{87}Sr/^{86}Sr$ of marine carbonates, both as a result of enhance rates of chemical weathering (Raymo and Ruddiman, 1992). These studies of Cenozoic uplifts make it reasonable to suppose that similar kinds of feedbacks existed in the Mesozoic. For example, high rates of exhumation could have produced very high elevations, which in turn could have intensified monsoonal precipitation. Enhanced exhumation would also provide a continuous source of sediment for rivers flowing into the foreland basin, thus filling accommodation space and possibly increasing rates of basin subsidence, particularly close to the margin of the upthrust highlands. Interestingly, the middle to late Cretaceous is also characterized by a decrease in pCO_2 (Fletcher et al., 2007), a global decrease in temperature from the early to late Cretaceous (Huber et al., 2002), and an increase in $^{87}Sr/^{86}Sr$ (Burke et al., 1982). Future research will hopefully clarify whether Mesozoic uplifts along the North American cordillera had geochemical and climatic feedbacks similar to those associated with the Cenozoic uplift of Tibet.

4.4. Variable intensity of the monsoon over time

Although this study was focused on the Campanian epoch, low $\delta^{18}O$ values of mid-Cretaceous paleosol siderites from along the coast of the WIS (Ufnar et al., 2004 and references therein), low $\delta^{18}O$ of precipitation predicted using global climate models (Poulsen et al.,

2007) and global climate model simulations in general (DeConto et al., 1999; Poulsen et al., 1999, 2007) suggest that monsoonal atmospheric circulation was also occurring earlier in the Cretaceous. The paleogeographic nature of western North America, however, began to change dramatically in the Maastrichtian epoch of the Cretaceous and in the Paleogene with the draining of the WIS to form the Mississippi and Hudson Embayments (Fig. 6). This southerly and northerly retreat of the shoreline would have removed the source of moisture 'fueling' intense monsoonal precipitation along the North American cordillera and, indeed, the simulated Paleogene monsoon of Sewall and Sloan (2006) does not penetrate as far to the north as the Campanian monsoon we simulate here. In addition, Cenozoic changes in elevation of the Cordillera associated with (1) the erosion and/or collapse of the Sevier fold and thrust belt, (2) the onset of major Laramide orogenesis into the Paleogene, and (3) the change from compressional to transform plate motion along the western margin of the North American plate, would have modified the spatial distribution and intensity of thermally driven, seasonal pressure changes over the highlands. As a result of these moisture source and elevation changes, it is very likely that the intensity of the monsoonal rainfall in this region changed over time until the present day.

Studies of the North American monsoon are ongoing, but it is possible to use published data to begin to address the question of how the monsoon changed over time. For example, bivalves have been analyzed from several sites in the Hell Creek Formation (HCF) of the Williston basin in Montana (Dettman and Lohmann, 2000; Fig. 6). Those from Trumbo Ranch and Seven Blackfoot Creek have estimated ages ranging from 66.01 to 66.27 Ma (Dettman and Lohmann, 2000), making them Maastrichtian in age and contemporaneous with the early stages of the Laramide orogeny. Although less detail is known about the sedimentological context of the bivalves from these sites, $\delta^{18}O$ of these bivalves cluster into two groups in a manner similar to the Campanian, with one having higher average $\delta^{18}O$ of -9.6 ± 0.3 ‰ (1σ), and one having lower average $\delta^{18}O$ of -18.0 ± 3.2‰ (1σ). As in the case of the Campanian, higher $\delta^{18}O$ values suggest that small catchments were recharged by local precipitation over the inland HCF landscape, while much lower $\delta^{18}O$ values suggest that larger rivers were recharged by high-elevation, monsoonal, precipitation.

Similar bimodal distributions in $\delta^{18}O$ of bivalves, with modes having average values of ~ −9 and −15‰, respectively, are also observed in Paleocene sediments of the Powder River basin (Dettman and Lohmann, 2000; Kohn and Dettman, 2007; Fig. 6). This distribution suggests continual monsoonal circulation, and that the Powder River basin was still proximal enough to the remnants of the retreating WIS (i.e. Mississippi Embayment) and that the Laramide uplift topography west of it was still significant enough that orographic uplift and air mass rainout was favorable. Further to the south, paleobotanical data from an early Paleocene site in the proximal Denver basin has been used to estimate that ~1.2 m of presumably monsoonal rainfall fell adjacent to the Front Range uplift, helping give rise to a diverse tropical rainforest (Johnson and Ellis, 2002). The location and intensity of precipitation in both of these Paleocene cases is consistent with GCM simulations of monsoonal circulation during this time (Sewall and Sloan, 2006). In contrast, Paleocene bivalves from the more westerly Bighorn basin are far less variable, with an average $\delta^{18}O$ of -11.3 ± 0.8‰ (1σ) (Dettman and Lohmann, 2000). This observation suggests that the influence of monsoonal precipitation may have been limited only to topography/basins proximal to remnants of the WIS. This conclusion is supported by data that indicate humid, coal-forming conditions along the eastern Laramide front but limited coal deposition in drier western basins (Dickinson et al., 1988; Johnson and Ellis, 2002) and simulation of wetter eastern basins and dryer western basins by Sewall and Sloan (2006).

By early Eocene time, bivalves from both the Powder River and Bighorn basins are characterized by a more normal distribution in $\delta^{18}O$ and relatively high average values of -10.2 ± 1.4‰ (1σ; not including outlier values of −15.8 and −14.1‰) and -11.1 ± 0.5‰ (1σ), respectively (Dettman and Lohmann, 2000). The greatly reduced isotopic variability, and the overall higher average $\delta^{18}O$ of bivalves from both basins, indicates that the monsoon continued to weaken throughout the Paleogene as (1) seaway retreat continued and/or (2) as topographic relief decreased in response to lower rates of Laramide uplift and the infilling of intermontane basins. Ongoing stable isotope studies of materials from both proximal and interior basin sediments in conjunction with AGCM simulations incorporating

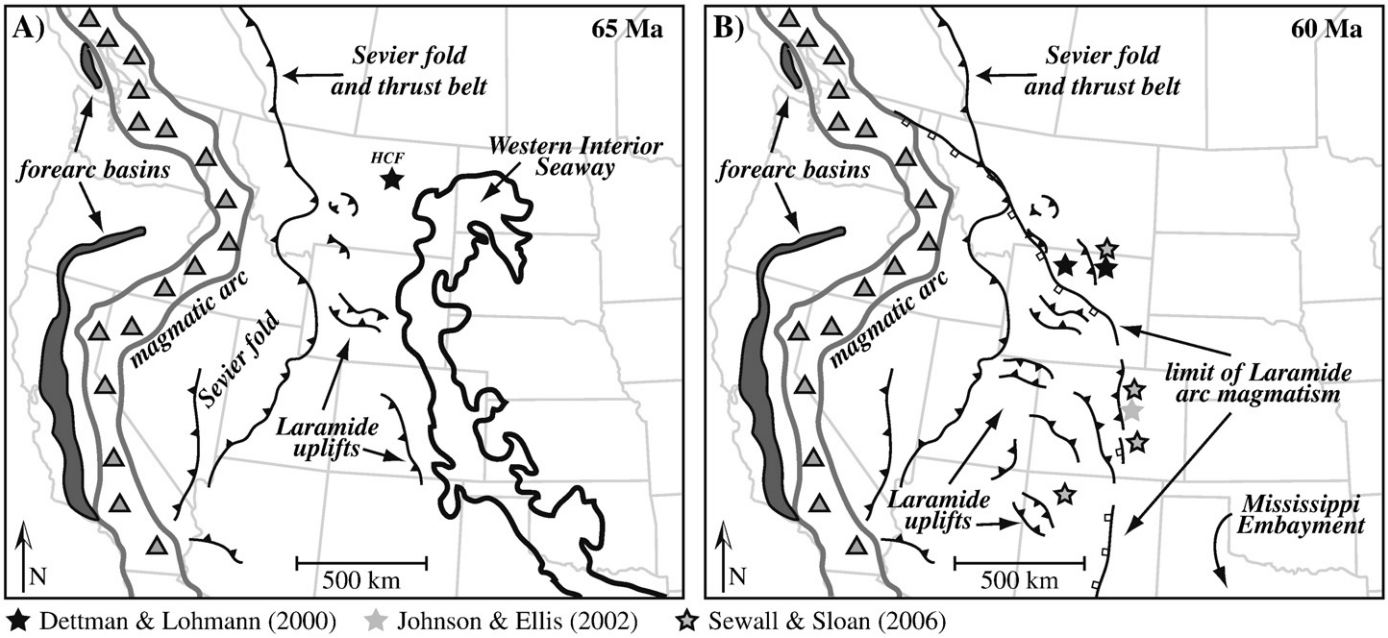

Fig. 6. A. Maastrichtian paleogeographic map of the Western Interior showing location of Williston basin sites discussed in texts. B. Paleogene paleogeographic map of the Western Interior showing locations of Bighorn, Denver, and Powder River basins discussed in text. Major tectonic features from Dickinson (2004) and seaway extent from Blakey (2008).

isotopic tracers should allow for a more detailed description of [atmospheric circulation patterns] wind directions, atmospheric moisture, and precipitation during this and younger time periods and the role played by paleoelevation.

5. Summary

Model simulations of Campanian wind directions and precipitation over North America indicate that a strong monsoon likely existed due to the close association of the Sevier highlands and the WIS. Oxygen isotope data from unionid bivalves and paleosol carbonates recovered from a ~10° latitude-wide section of the foreland basin reveal a spatial pattern that is consistent with such east to west movement of water vapor from low to high elevations, and subsequent recharge of foreland basin rivers by high-elevation precipitation. Because of focused seasonal precipitation in the highlands, oxygen isotope ratios from this region cannot be considered a global average. The recognition of monsoonal precipitation raises the intriguing possibility that climate influenced tectonic uplift of the western highlands.

Acknowledgements

Financial support was provided to HCF by National Science Foundation EAR-#0319041, American Chemical Society-Petroleum Research Fund #38141-GB8, and Colorado College, and to BZF by a Geological Society of America Research Grant (2007) and a NSF Graduate Research Fellowship. R.R. Rogers, D. W. Boyd, E. M. Roberts and L. Tapanila assisted in obtaining bivalve specimens. L. Wingate and S. Sharma are thanked for laboratory assistance. Helpful reviews of this manuscript were provided by D. Fox, C. Poulsen, and two anonymous reviewers.

Appendix A. Supplementary data

Supplementary data associated with this article can be found, in the online version, at doi:10.1016/j.epsl.2009.10.018.

References

Araguas-Araguas, L., Froehlich, K., Rozanski, K., 1998. Stable isotope composition of precipitation over southeast Asia. J. Geophys. Res. 103, 28721–28742.
Blakey, R., 2008. Paleogeography and Geologic Evolution of North America. http://jan.ucc.nau.edu/~rcb7/nam.html.
Bryson, R.A., Hare, R.K., 1974. The climate of North America. In: Bryson, R.A., Hare, R.K. (Eds.), Climates of North America (World survey of climatology, volume 11). Elsevier, New York, pp. 1–47.
Burke, W.H., Denison, R.E., Hetherington, E.A., Koepnick, R.B., Nelson, H.F., Otto, J.B., 1982. Variation of seawater 87Sr/86Sr throughout Phanerozoic time. Geology 10, 516–519.
Carpenter, K., 1987. Paleoecological significance of droughts during the Late Cretaceous of the Western Interior. In: Koster, E.H. (Ed.), Fourth Symposium on Mesozoic Terrestrial Ecosystems, pp. 42–47.
Collins, W.D., Rasch, P.J., Boville, B.A., Hack, J.J., McCaa, J.R., Williamson, D.L., Briegleb, B.P., Bitz, C.M., Lin, S.J., Zhang, M.H., 2006. The formulation and atmospheric simulation of the Community Atmosphere Model version 3 (CAM3). J. Climate 19, 2144–2161.
Dansgaard, W., 1964. Stable isotopes in precipitation. Tellus 16, 436–468.
DeCelles, 2004. Late Jurassic to Eocene evolution of the Cordilleran thrust belt and foreland basin system, western U.S.A. Am. J. Sci. 304, 105–168.
DeConto, R.M., Brady, E., Bergengren, J.C., Thompson, S.L., Pollard, D., Hay, W.W., 1999. Late Cretaceous climate, vegetation, and ocean interactions. In: Huber, B., MacLeod, K.G., Wing, S.L. (Eds.), Warm Climates in Earth History. Cambridge University Press, pp. 275–297.
Dettman, D.L., Lohmann, K., 2000. Oxygen isotope evidence for high-altitude snow in the laramide Rocky Mountains of North America during the Late Cretaceous and Paleogene. Geology 28, 243–246.
Dickinson, W.R., 2004. Evolution of the North American Cordillera. Annu. Rev. Earth Planet. Sci. 32, 13–45.
Dickinson, W.R., Klute, M.A., Hayes, M.J., Janecke, S.U., Lundin, E.R., McKittrick, M.A., Olivares, M.D., 1988. Paleogeographic and paleotectonic setting of Laramide sedimentary basins in the central Rocky Mountain region. Geol. Soc. Am. Bull. 100, 1023–1039.
Dutton, A., Wilkinson, B.H., Welker, J.M., Bowen, G.J., Lohmann, K.C., 2005. Spatial distribuiton and seasonal variation in $^{18}O/^{16}O$ of modern precipitation and river water across the conterminous USA. Hydrol. Process. 19, 4121–4146.
Eberth, D.A., 2005. The Geology. In: Currie, P.J., Koppelhus, E.B. (Eds.), Dinosaur Provincial Park: A Spectacular Ancient Ecosystem Revealed. Indiana University Press, Bloomington, pp. 54–87.
Eberth, D.A., Getty, M.A., 2005. Ceratopsian bonebeds: Occurrence, origins and significance. In: Currie, P.J., Koppelhus, E.B. (Eds.), Dinosaur Provincial Park: A specatular ancient ecosystem revealed. Indiana University Press, Bloomington, pp. 501–536.
Eberth, D.A., Hamblin, A.P., 1993. Tectonic, stratigraphic, and sedimentological significance of a regional discontinuity in the Upper Judith River Group (Belly River wedge) of southern Alberta, Saskatchewan, and northern Montana. Can. J. Earth Sci. 30, 174–200.
Eberth, D. A., D. B. Brinkman, and V. Barkas. in press. A centrosaurine mega-bonebed from the Upper Cretaceous of southern Alberta: Implications for behaviour and death events. In M. J. Ryan, B. J. Chinnery-Allgeier, and D. A. Eberth (eds.), New Perspectives on Horned Dinosaurs. Bloomington: Indiana University Press.
Falcon-Lang, H.J., 2003. Growth interruptions in conifer woods from the Upper Cretaceous (Campanian) Two Medicine Formation, Montana, USA: implications for palaeoclimate and dinosaur ecology. Palaeogeogr. Palaeoclimatol. Palaeoecol. 199, 299–331.
Fletcher, B.J., Brentnall, S.J., Anderson, C.W., Berner, R.A., Beerling, D.J., 2007. Atmospheric carbon dioxide linked with Mesozoic and early Cenozoic climate change. Nat. Geosci. 1, 43–48.
Foreman, B.Z., Rogers, R.R., Deino, A.L., Wirth, K.R., Thole, J.T., 2008. Geochemical characterization of bentonite beds in the Two Medicine Formation (Campanian, Montana), including a new $^{40}Ar/^{39}Ar$ age. Cretac. Res 29 (3), 373–385.
Fricke, H.C., Rogers, R.R., Backlund, R., Dwyer, C.N., Echt, S., 2008. Preservation of primary stable isotope signals in dinosaur remains, and environmental gradients of the Late Cretaceous of Montana and Alberta. Palaeogeogr. Palaeoclimatol. Palaeoecol. 266, 13–27.
Fricke, H.C., Rogers, R.R., Gates, T., 2009. Hadrosaurid migration: inferences based on stable isotope comparisons among Late Cretaceous dinosaur localities. Paleobiology 35, 270–288.
Friedman, I., O'Neil, J.R., 1977. Compilation of stable isotope fractionation factors of geochemical interest. In: Fleischer, M. (Ed.), Data of Geochemistry: U.S. Geological Survey Professional Paper, vol. 440-KK, pp. 1–12.
Gat, J.R., 1996. Oxygen and hydrogen isotopes in the hydrologic cycle. Annu. Rev. Earth Planet. Sci. 24, 225–262.
Gill, J.R., Cobban, W.A., 1973. Stratigraphy and geologic history of the Montana Group and equivalent rocks, Montana, Wyoming, and North and South Dakota. US Geol. Surv. Prof. Pap. 776, 37.
Gradstein, F.M., Ogg, J.G., Smith, A.G., et al., 2004. A geologic time scale. Cambridge University Press.
Heydenburg, R.J., 1966. Stratigraphy and depositional environments of the Parkman Sands Member, Mesaverde Formation, near Midwest, Natrona County, Wyoming. M.Sc. University of Wyoming, Laramie, Wyoming, p. 81.
Hippe, D.J., Needham, D.W., Ethridge, F.G., 1986. Depositional systems and petroleum potential, Mesaverde Formation, southeastern Wind River basin, Wyoming. AAPG Bulletin 70 (8), 1043–1044.
Huber, B.T., Norris, R.D., MacLeod, K.G., 2002. Deep sea paleotemperature record of extreme warming during the Cretaceous. Geology 30, 123–126.
Jerzykiewicz, T., Sweet, A.R., 1987. Semiarid floddplain as a paleoenvironmental setting of the Upper Cretaceous dinosaurs: sedimentological evidence from Mongolia and Alberta. In: Currie, P.J., Koster, E.H. (Eds.), Fourth Symposium on Mesozoic Terrestrial Ecosystems, pp. 125–128.
Jerzykiewicz, T., Sweet, A.R., 1988. Sedimentological and palynological evidence of regional climatic changes in the Campanian to Paleocene sediments of the Rocky Mountain Foothills, Canada. Sediment. Geol. 59, 29–76.
Johnson, K.R., Ellis, B., 2002. A tropical rainforest in Colorado 1.4 million years after the Cretaceous–Tertiary Boundary. Science 296, 2379–2383.
Kohn, M., Dettman, D.L., 2007. Paleoaltimetry from stable isotope compositions of fossils. In: Kohn, M. (Ed.), Paleoaltimetry: Geochemical and thermodynamic approaches. Reviews in Mineralogy and Geochemistry, vol. 66. Mineralogical Society of America, pp. 119–154.
Kump, L.R., Slingerland, R.L., 1999. Circulation and stratification of the early Turonian Western interior seaway: sensitivity to a variety of forcings. In: Johnson, C.C. (Ed.), Evolution of the Cretaceous ocean –climate system, pp. 181–190.
Kutzbach, J.E., Guetter, P.J., Ruddiman, W.F., Prell, W.L., 1989. Sensitivity of climate to late Cenozoic uplift in southern Asia and the American west — numerical experiments. J. Geophys. Res.-Atmos. 94, 18393–18407.
Ludvigson, G.A., Gonzalez, L.A., Metzger, R.A., Witzke, B.J., Brenner, R.L., Murillo, A.P., White, T.S., 1998. Meteoric sphaerosiderite lines and their use for paleohydrology and paleoclimatology. Geology 26, 1039–1042.
Otto-Bliesner, B.L., Brady, E.C., Shields, C., 2002. Late Cretaceous ocean: coupled simulations with the National Center for Atmospheric Research Climate System Model. J. Geophys. Res.-Atmos. 107. doi:10.1029/2001JD000821.
Poulsen, C.J., Barron, E.J., Johnson, C.C., Fawcett, P.J., 1999. Links between the major climatic factors and regional oceanography in the mid-Cretaceous. In: Barrera, E., Johnson, C.C. (Eds.), Evolution of the Cretaceous ocean –climate system, pp. 73–90.
Poulsen, C.J., Pollard, D., White, T.S., 2007. GCM simulation of the $\delta^{18}O$ content of continental precipitation in the middle Cretaceous: a model-proxy comparison. Geology 35, 199–202.
Raymo, M.E., Ruddiman, W.F., 1992. Tectonic forcing of late Cenozoic climate. Nature 359, 117–122.
Reiners, P.W., Ehlers, T.A., Mitchell, S.G., Montgomery, D.R., 2003. Coupled spatial variations in precipitation and long-term erosion rates across the Washington Cascades. Nature 426, p645–p647.
Reiter, E.R., Tang, M., 1984. Plateau effects on diurnal circulation patterns. Mon. Weather Rev. 112, 638–651.

Roberts, E.M., 2007. Facies architecture and depositional environments of the Upper Cretaceous Kaiparowits Formation, southern Utah. Sedimentary Geology 197, 207–233.
Roberts, E.M., Deino, A.L., Chan, M.A., 2005. $^{40}Ar/^{39}Ar$ age of the Kaiparowits Formation, southern Utah, and correlation of contemporaneous Campanian strata and vertebrate faunas along the margin of the Western Interior Basin. Cretaceous Research 26, 307–318.
Rogers, R.R., 1990. Taphonomy of three dinosaur bone beds in the Upper Cretaceous Two Medicine Formation of Montana: evidence for drought-related mortality. Palaios 5, 394–413.
Rogers, R.R., 1993. Systematic patterns of time-averaging in the terrestrial vertebrate record: a Cretaceous case study. In: Kidwell, S.M., Behrensmeyer, A.K. (Eds.), Taphonomic Approaches to Time Resolution in Fossil Assemblages. Short Courses in Paleontology. The Paleontological Society, pp. 228–249.
Rogers, R.R., 1998. Sequence analysis of the Upper Cretaceous two medicine and Judith River formations, Montana: nonmarine response to the Claggett and Bearpaw marine cycles. J. Sediment. Res. 68, 615–631.
Rogers, R.R., Brady, M.E. in press. Origins of microfossil bonebeds: insights from the Upper Cretaceous Judith River Formation of north-central Montana. Paleobiology.
Rogers, R.R., Kidwell, S.M., 2000. Associations of vertebrate skeletal concentrations and discontinuity surfaces in terrestrial and shallow marine records: a test in the Cretaceous of Montana. J. Geol. 108, 131–154.
Rogers, R.R., Swisher III, C.C., Horner, J.R., 1993. $^{40}Ar/^{39}Ar$ age and correlation of the nonmarine Two Medicine Formation (Upper Cretaceous), northwestern Montana, U.S.A. Can. J. Earth Sci. 30, 1066–1075.
Rowley, D.B., 2007. Stable isotope-based paleoaltimetry: theory and validation. In: Kohn, M. (Ed.), Paleoaltimetry: geochemical and thermodynamic approaches, pp. 23–52.
Rozanski, K., Araguás-Araguás, L., Gonfiantini, R., 1993. Isotopic patterns in modern global precipitation. In: Swart, P.K., Lohmann, K.C., McKenzie, J., Savings, S. (Eds.), Climate Change in the Continental Isotopic Records. American Geophysical Union, Washington, D.C., pp. 1–36.
Ruddiman, W.F., Kutzbach, J.E., 1989. Forcing of late Cenozoic Northern Hemisphere climate by plateau uplift in southern Asia and the American west. J. Geophys. Res.-Atmos. 94, 18409–18427.
Sewall, J.O., Sloan, L.C., 2006. Come a little bit closer: a high-resolution climate study of the early Paleogene Laramide foreland. Geology 34, 81–84.
Sewall, J.O., Sloan, L.C., Huber, M., Wing, S.L., 2000. Climate sensitivity to changes in land surface characteristics. Glob. Planet. Change 26, 445–465.
Sewall, J.O., van de Wal, R.S.W., van der Zwan, K., van Oosterhout, C., Dijkstra, H.A., Scotese, C.R., 2007. Climate model boundary conditions for four Cretaceous time slices. Clim. Past 3, 647–657.
Ufnar, D.F., González, L.A., Ludvigson, G.A., Brenner, R.L., Witzke, B.J., 2002. The mid-Cretaceous water bearer: isotope mass balance quantification of the Albian hydrologic cycle. Palaeogeogr. Palaeoclimatol. Palaeoecol. 188, 51–71.
Ufnar, D.F., Gonzalez, L.A., Ludvigson, G.A., Brenner, R.L., Witzke, B.J., 2004. Evidence for increased latent heat transport during the Cretaceous (Albian) greenhouse warming. Geology 32, 1049–1052.
White, T.S., Gonzalez, L.A., Ludvigson, G.A., Poulsen, C., 2001. Middle Cretaceous greenhouse hydrologic cycle of North America. Geology 29, 363–366.
Willett, S.D., 1999. Orogeny and orography: the effects of erosion on the structure of mountain belts. J. Geophys. Res. 104, 28957–28982.
Wobus, C.W., Hodges, K.V., Whipple, K.X., 2003. Has focused denudation sustained active thrusting at the Himalayan topographic front? Geology 31, 861–864.
Wolfe, J.A., Upchurch, G.R., 1987. North American nonmarine climates and vegetation during the late Cretaceous. Palaeogeogr. Palaeoclimatol. Palaeoecol. 61, 33–77.
Zhisheng, A., Kutzbach, J.E., Prell, W.L., Porter, S.C., 2001. Evolution of Asian monsoons and phased uplift of the Himalaya–Tibetan plateau since Late Miocene times. Nature 411, 62–66.